International Journal of Heat and Mass Transfer 115 (2017) 430–440

Contents lists available at ScienceDirect

International Journal of Heat and Mass Transfer

journal homepage: www.elsevier.com/locate/ijhmt

Natural convection heat transfer in a nanofluid-filled cavity with double sinusoidal wavy walls of various phase deviations

Wenhui Tang [a], M. Hatami [a,b], Jiandong Zhou [a], Dengwei Jing [a,*]

[a] International Research Center for Renewable Energy, State Key Laboratory of Multiphase Flow in Power Engineering, Xi'an Jiaotong University, Xi'an 710049, China
[b] Department of Mechanical Engineering, Esfarayen University of Technology, Esfarayen, North Khorasan, Iran

ARTICLE INFO

Article history:
Received 12 April 2017
Received in revised form 17 June 2017
Accepted 4 July 2017
Available online 22 July 2017

Keywords:
Nanofluids
RSM
Convection coefficient
Phase deviation
Sinusoidal wavy walls

ABSTRACT

In the present study, a new 2D quarter-circular enclosure with two sinusoidal wavy walls and two straight walls was proposed. Natural convection heat transfer in such cavities filled with various kinds of nanofluids was investigated and the phase deviation between two sinusoidal wavy walls was paid special attention. With the given shape of inner wall, the effect of shape regulation of the outer wavy wall was studied by a combined Finite volume method (FVM) and response surface method (RSM) method. Sinusoidal amplitude of outer wall (A) and phase deviation (γ) between the inner and outer walls were found to have significant effects on surface heat transfer coefficient h. The isothermal lines deform and fluctuate much more intensively with the increase of γ. RSM optimization manifested that the highest h appears at $A = 0.11$ and $\gamma = 1.77$ rad for water-Ag nanofluid. In the optimal enclosure, the surface heat transfer coefficient increases as the volume fraction of nanofluid increases. With the increasing of Ra, mass flow rate increases greatly. Water-Ag, water-CuO, water-Al_2O_3, water-TiO_2 nanofluids have been studied and it shows that water-Ag nanofluid has higher surface heat transfer coefficient than the others. For the cavity with double sinusoidal wavy walls, a periodical fluctuation of local Nusselt number at different locations of the outer wavy wall has been found and the net result is that the outer wall Nusselt number is evidently larger than that with only single sinusoidal wavy wall.

1. Introduction

Natural convection heat transfer in a cavity induced by temperature and density gradients has found various promising applications such as in electronic devices, aerospace and automotive industry [1–4]. The physics of natural convection in cavities (circular, rectangular, etc.) has many applications especially in solar collectors, in special design of two-walled windows. It is also widely applied in heat exchanger, caliduct, nuclear reactor cooling pipes and so on. Therefore, enhancing the heat transfer efficiency in cavity is the key issue for these applications. Nanofluids, or nanoparticle suspensions, have attracted increasing attention in recent years for their excellent performance compared to its base liquid when applied in heat and mass transfer [5–7]. In this respect, replacing of the initial pure liquid in cavity by an appropriate nanofluid has been widely attempted and it is expected that the addition of the nanoparticles could significantly increase the thermal conductivity, Nusselt number and surface heat transfer coefficient of the working fluid in the designed cavity.

Kefayati et al. have investigated in detail natural convection heat transfer in nanofluid using Lattice Boltzmann Method [8–13]. Study on turbulent natural convection in tall enclosures using Cu/Water nanofluid using Lattice Boltzmann Method shows that the increment of the aspect ratio causes heat transfer to decline in different Rayleigh numbers. The effects of a magnetic field on natural convection flow in filled long enclosures with Cu/water nanofluid have also been analyzed by lattice Boltzmann method [9]. It shows that heat transfer decreases with the growth of the aspect ratio but this growth causes the effect of the nanoparticles to increase. Kefayati et al. studied the two-dimensional steady mixed convection in a square enclosure with differentially heated sidewalls [13]. Heat transfer and entropy generation on laminar natural convection of non-Newtonian nanofluids in a porous square cavity have been analyzed by Finite Difference Lattice Boltzmann Method (FDLBM) [14]. Results indicated that heat transfer and different irreversibilities enhance as Rayleigh number increases. The enhancement of the volume fraction augments heat transfer and the entropy generations due to heat transfer and fluid friction. Natural convection and entropy generation of non-Newtonian nanofluid have also been investigated using the Finite Difference Lattice Boltzmann method (FDLBM) [15]. The total

* Corresponding author.
E-mail address: dwjing@mail.xjtu.edu.cn (D. Jing).

http://dx.doi.org/10.1016/j.ijheatmasstransfer.2017.07.057
0017-9310/

Nomenclature

a	amplitude (m)
A	A = 2A′ for convenience
A'	dimensionless amplitude
C_p	heat capacity (J/kg K)
F	total force acting on nanoparticle (N)
g	gravitational acceleration (m/s^2)
h	surface heat transfer coefficient (convection coefficient) (W/m^2 K)
I	unit vector
k	thermal conductivity (W/m K)
m	mass (kg)
N	number of sinusoidal undulations
Nu	Nusselt number
Pr	Prandtl number
r	radius of spherical nanoparticle (m)
Ra	Rayleigh number
S_p	source term
t	time (s)
T	temperature (K)
v	velocity (m/s)

Greek symbols

τ	stress tensor (Pa)
B	thermal expansion coefficient (K^{-1})
γ	phase deviation (rad)
ζ	Rotation angle with respect to horizontal plane (°)
φ	volume fraction
ρ	Density (kg/m^3)
ν	kinematic viscosity (m^2/s)
μ	shear viscosity (Pa s)

Subscripts

ave	average
c	cold wall
h	hot wall
in	inner wall
l	pure water
loc	local
p	particle
v	virtual mass
out	outer wall

entropy generation increases as the buoyancy ratio number augments. It was shown that the increase in the Brownian motion and Thermophoresis parameters enhances the total irreversibility.

Magneto-hydrodynamic(MHD) flow has also been given particular attention [16–20]. Khan et al. studied the shape effect of nanoparticle on heat transfer in magneto-hydrodynamic flow [16]. It is noticed that the temperature of the fluid is maximum for the platelet-shaped particles followed by the cylinder- and brick-shaped particles. Magneto-hydrodynamic effects are incorporated along with the passive control model of nanofluids that also takes into account the Brownian motion and thermophoresis effects in their another study [17]. Kefayati investigated the effect of a magnetic field on natural convection flow in a nanofluid-filled cavity with sinusoidal temperature distribution on one side wall [19]. He also simulated heat transfer and entropy generation of MHD natural convection of non-Newtonian nanofluid in an enclosure [20]. It is noted that the augmentation of the power-law index causes heat transfer to drop in the absence of the magnetic field, by contrast, the heat transfer increases with the rise of power-law index in the presence of the magnetic field. Besides, Nanofluid heat transfer characteristics have been studied when it flow in different channels and cavities [21,22]. Khan et al. studied heat transfer effects of carbon nanotubes suspended nanofluid flow in a channel with non-parallel walls [21]. They also conducted numerical investigation for three dimensional squeezing flow of nanofluid in a rotating channel with lower stretching wall [22]. We have employed a response surface methodology (RSM) combined with FEM methods to find an optimal performance for a circular-wavy cavity (CWC) filled by nanofluid under the natural convection heat transfer condition [23]. The results show that the effect of Lewis number on Nusselt number can be considered significant only for the high buoyancy ratio numbers. As for the geometry of the cavity, natural convection in circular-wavy cavity has been studied by Sheikholeslami et al. [24]. Sheikholeslami studied the heat transfer characteristics when the inner wall amplitude is 0.2 and the undulation number is 2. By using RSM it is found that the optimal amplitude of 0.3 and undulation number of 3 for such enclosure. Sheremet et al. investigated the natural convective heat transfer and nanofluid flow in a cavity with top wavy wall and corner heater. It was found that nanoparticle volume fraction essentially affects both fluid flow and heat transfer while undulation number only significantly changes the heat transfer rate [25]. Further study of such kind of enclosure was conducted by Motlagh et al. using Buongiorno's two-phase model [26]. It was found that the inclination of such enclosure can greatly enhance the Nusselt number. Buongiorno's two-phase model is also used by Kefayati et al. in mixed convection [27]. Moreover, Esfandiary et al. investigated natural convection of Al_2O_3-water nanofluid in an inclined enclosure considering the effect of Brownian motion and thermophoresis and the highest value for Nusselt number has been achieved when the inclination angle of the cavity is 30° [28].

In spite of many studies on natural convection heat transfer of nanofluids in various cavities, more numerical and experimental investigations on cavity of various geometries are still needed considering the very complicated conditions and rigorous requirements during their practical applications [27–29]. Besides the work introduced above, Rostami et al. also found that the Nusselt number for the wavy micro-channel is larger than that for flat walls micro-channels [30]. There is an optimal geometry for wavy-walls micro-channels which leads to the maximum Nusselt number. Deng et al. studied natural convection in a rectangular enclosure with sinusoidal temperature distributions on both side walls [31]. The results showed that the natural-convection heat transfer in enclosures with sinusoidal temperature distributions on both walls is superior to that with the sinusoidal temperature distribution only on one side. In their study, phase deviation of the sinusoidal temperature distributions on the two side walls are also taken into consideration and found to be crucial for the enhancement of heat transfer of the cavity. Alsabery et al. have investigated the conjugate natural convection in a square cavity filled with nanofluid which has sinusoidal temperature variations on both horizontal walls [32]. They found that the streamlines, isotherms and heatlines can be significantly affected by phase deviation of two sinusoidal temperature profiles. The heat transfer performance at outer wall can be enhanced by simply changing the phase deviation of temperature distribution at two walls without increasing the total volume of cavity. As mentioned above, circular-wavy cavity (CWC) has been studied by Sheikholeslami et al. [24] and us [23] and the significantly improved heat transfer performance has been achieved over such geometry. In our previ-

ous study, a sinusoidal wavy structure of microchannel heat sink intended for active cooling of compact electronic devices has also been designed. For our optimized wavy channel, the heat transfer can be enhanced by a maximum of 2.8 times compared to regular straight channel. In such case, the heat transfer enhancement also outweighs the increased pressure drop [33].

The above work inspires us to study the heat transfer efficiency of the cavity when both the inner and outer walls of the cavity possess sinusoidal wavy structures, that is, a wavy-wavy cavity (WWC). As is well known, for the fabrication of compact and precise devices, cooling units as small as possible are always preferred. Sometimes reduction of heat transfer resistance even overweighs the pressure drop when the compactness and precision of the devices are the priority. Compared to circular outer wall, a sinusoidal wall is expected to be space-saving and may have higher heat transfer efficiency [34]. Besides, phase deviation can also be taken into consideration for such geometry for its potential to enhance heat transfer [34,35]. In the present study we will try to find the optimal shape of outer wall for such WWC geometry and discuss how phase deviation of two wavy walls influences the surface heat transfer coefficient on outer wall, which to our knowledge has not yet been considered in the previous work.

It is worth noting here that previous study has reported a circular-wavy cavity(CWC) [23]. However, in our present work it is a wavy-wavy cavity (WWC). In such cases, both the inner and outer walls of the cavity are sinusoidal. It thus becomes possible to investigate the effect of phase difference between the inner and outer walls besides the amplitude of the walls. In the present study, a two-dimensional quarter circular cavity with two wavy walls has been employed to investigate the natural convection heat transfer process in the presence of four kinds of nanofluids, i.e. water-TiO_2, water-Al_2O_3, water-Ag, and water-CuO, respectively. RSM and finite volume method (FVM) will be applied for the finding of the optimal cavity shape with special attention paid to the optimization of the phase deviation for the two wavy walls. There are mainly four parts in this study. Firstly, we assume that amplitude of inner wavy wall is 0.3 with an undulation number of 3. Four kinds of nanofluids will then be investigated under 9 combinations of amplitude and phase deviation. Next, response surface method (RSM) and FVM are used to find the optimal amplitude of the outer wall and phase deviation to achieve the highest surface heat transfer coefficient of outer wall. Finally, the effect of nanoparticle volume fraction and *Ra* on surface heat transfer coefficient will be discussed. As will be shown, a significant improvement in outer wall Nusselt number has been obtained compared to our previous work [23]. It is also found that this improvement can both enhance heat transfer efficiency and the compactness of the device for practical applications as well.

2. Geometry definition and boundary conditions

The problem being considered is based on the previous study of Sheikholeslami et al. [24] and ours [23]. As schematically shown in Fig. 1, a two-dimensional quarter circular cavity with two wavy walls has been established to investigate the natural convection heat transfer process over four different kinds of nanofluids. The corresponding quadrilateral dominant meshes used in the present FVM program are displayed in Fig. 2. The inner and outer walls are maintained at constant temperatures T_h and T_c, respectively. The other two boundaries are adiabatic. The shape of inner and outer wavy walls is assumed to mimic the following pattern:

$$\mathrm{r} = \mathrm{r_{in}} + \mathrm{A}\cos(\mathrm{N}(\zeta)) \tag{1}$$

$$\mathrm{r} = \mathrm{r_{out}} + \mathrm{A}\cos(\mathrm{N}(\zeta)) \tag{2}$$

where r_{in} and r_{out} are the initial circle radii of inner and outer walls, A and N are amplitude and number of undulations, respectively, and ζ is the rotation angle with respect to the horizontal plane. In the present study, for simplification, it is assumed that A and N of inner wall keeps to 0.3 and 9, respectively, which has been determined by our previous work to be optimized [23]. The amplitude and undulation number for the outer wall are unknown and will be optimized by RSM. The number of boundary layer is five and maximum cell size is 0.01. Totally, there are 9 meshes developed by auto method and we assume that mesh quality is beyond 0.5 which means our meshes are of desired quality for further calculation.

3. Mathematical modeling and numerical procedure

3.1. Problem formulation

The wavy-wavy enclosure in the present study is based on and transformed from a quarter of cyclic annular cavity with a 9 μm inner radius and a 20 μm outer radius. The governing equations are calculated under Eulerian frame while the nanoparticle is tracked using Lagrangian model. The volume fraction parameters are calculated under implicit scheme. The primary phase is liquid water and the secondary phase is various kinds of nanoparticles with an averaged diameter of 20 nm. The Pressure-velocity coupling equation uses phase coupled SIMPLE scheme. All cases converge within 1000 steps.

3.1.1. Governing equations of the continuous phase

The equations for laminar natural convection under Eulerian model are based on the Ansys-Fluent Theory Guide [34] Thermophoretic and Brownian forces are not included in the present study. The equations that describe the movement of continuous phase are based on a previous work from He et al. [35]:

Continuity equation:

$$\frac{\partial \rho}{\partial t} + \nabla \cdot (\rho V) = 0 \tag{3}$$

Momentum Equation:

$$\frac{\partial}{\partial t}(\rho_l v_l) + \nabla \cdot (\rho_l v_l v_l) = -\nabla p + \nabla \cdot \tau_l + \rho_l g - S_p \tag{4}$$

where S_p can be obtained by:

$$S_p = \sum \mathrm{Fm_p}\Delta t \tag{5}$$

Energy Equation:

$$\rho_l c\left[\frac{\partial \tau}{\partial t} + v_l \cdot \nabla \tau\right] = \nabla \cdot (k \nabla \tau) \tag{6}$$

where τ_1 can be obtained by:

$$\tau_l = \mu_l\left[\nabla v_l + \nabla v_l^T\right] - \frac{2}{3}\mu_l \nabla \cdot v_l I \tag{7}$$

Eqs. (3)–(7) describe the movement of continuous water phase. ρ_l is the fluid density, v_l the velocity, t the time, p the pressure, g the gravitational acceleration, c the heat capacity, k the thermal conductivity, and T is the fluid temperature, Here, τ is stress tensor, F the total force acting on a particle, I the unit vector and m_p is the mass of nanoparticle.

3.1.2. Equations of nanoparticles

The equations that describe the movement of nanoparticles are based on a previous work from He et al. [35]. However, the effect of Brownian force and thermopheretic force has not been taken into condition. He et al. have conducted numerical studies for laminar

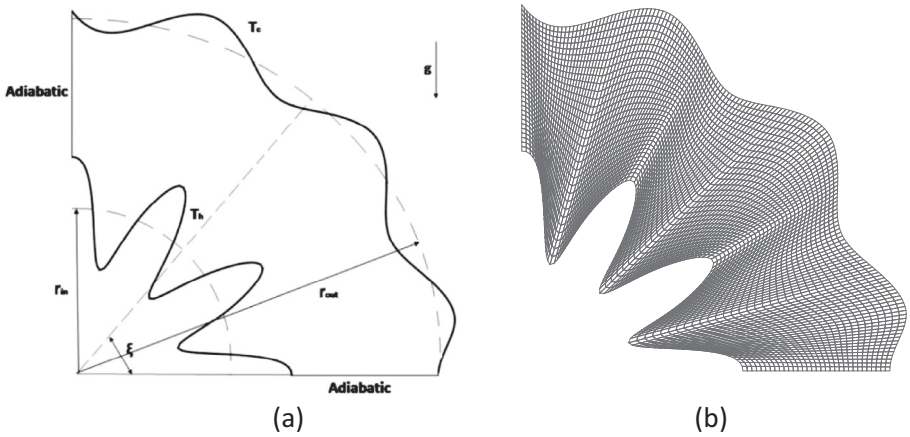

Fig. 1. Physical model for the wavy-wavy cavity (WWC) cavity (a) and the quadrilateral mesh for the calculated domain when γ = 1.77 rad, A = 0.11 (b).

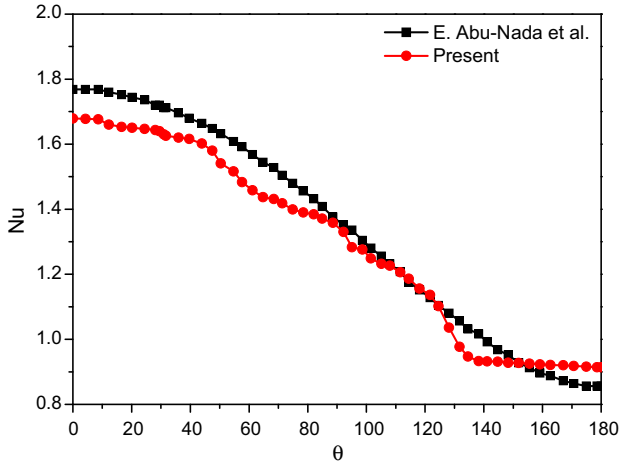

Fig. 2. Validation of the model accuracy with the data available in the literature from Abu-Nada et al. [41].

flow with and without considering the thermophoretic and Brownian forces, and concluded that these two forces have negligible effect on the heat transfer characteristics. Therefore, in order to simplify our model, we ignored the effect of Brownian force and thermophoretic force [35].

In Lagrangian frame of reference, the equation of motion of a nanoparticle is as follows:

$$\frac{\mathrm{d}v_p}{dt} = F \tag{8}$$

Here, F can be written as:

$$F = F_D + F_G + F_L + F_P + F_V \tag{9}$$

where F_D is the hydrodynamic drag force from the fluid, F_G is the force due to gravity and F_L the Staffman's lift force, F_P is the force due to gravity gradient and F_V the virtual mass force. There forces can be calculated by following equations Eqs. (10)–(14), respectively.

F_D can be derived by applying the Stokes' law [36]:

$$F_D = 6\pi\mu_l r_i(u_i - u_p) \tag{10}$$

F_G can be obtained by:

$$F_G = \frac{g(\rho_p - \rho_l)}{\rho_p} \tag{11}$$

The Staffman lift force due to shear field, F_L, has been derived by Staffman [37]:

$$F_L = \frac{2K_S v^{1/2}\rho_l d_{ij}}{\rho_p d_p (d_{lk}d_{kl})^{1/4}}(v_l - v_p) \tag{12}$$

where K_s = 2.594 is a constant, d_{ij} is the deformation tensor defined as $d_{ij} = 1/2(v_l^{ij}+v_l^{j,i})$ and F_P is the force due to gravity gradient:

$$F_P = \left(\frac{\rho_l}{\rho_p}\right) v_p \cdot \nabla v_l \tag{13}$$

F_V is virtual mass force:

$$F_V = \frac{1}{2}\frac{\rho_l}{\rho_p}\frac{d}{dt}(v_l - v_p) \tag{14}$$

$$\mathrm{h} = \frac{k_{nf}\left(\frac{\partial T}{\partial r}\right)_{out}}{T_{\mathrm{out}} - T_{ave}} \tag{15}$$

where h is surface heat transfer coefficient. $(\partial T/\partial \mathrm{r})_w$ denotes the radial temperature gradient at the wall. T_{out} and T_{ave} are the outer wall temperature and the average temperature across the cavity cross-section at a given ζ, respectively.

3.2. Assumption and simplification

1. The working fluid, which is nanofluid in our study, is considered as incompressible laminar flow across a cavity and maintains the condition of single phase.
2. The thermophysical properties of the nanoparticle are constant.
3. The two straight surface of the cavity is well insulated.
4. The diameter of nanoparticles is uniform for every nanoparticle.

3.3. Thermo-physical properties of nanofluids

The thermo-physical properties of pure water and Ag, CuO, Al_2O_3 and TiO_2 are obtained from literature [38] and are also listed in Table 1. Here, nanofluid is the mixture of water and Ag/CuO/Al_2O_3/TiO_2 nanoparticles.

3.4. Gird and independence test

In order to obtain accurate results and reduce calculation, grid independence tests have been conducted with pure water as working fluid in the WWC cavity when γ = 0, A = 0.1. The results are presented in Table 2. Considering both timesaving and accuracy, mesh number of 16,678 was chosen for our calculation. Note that since

Table 1
Thermo-physical properties of pure water and Ag, CuO, Al_2O_3 and TiO_2 nanoparticles.

Physical properties	Water	Ag	CuO	Al_2O_3	TiO_2
Cp (J/kg K)	4179	235	383	765	686.2
ρ (kg/m^3)	998.2	10,500	8954	3600	4250
K (W/m K)	0.6	429	400	46	8.954
B (K^{-1})	2.1×10^{-4}	1.95×10^{-5}	1.80×10^{-5}	0.85×10^{-5}	0.9×10^{-5}

Table 2
Gird testing for Nusselt number at different mesh number for $\gamma = 0$, $A = 0.1$.

Mesh number	*h*(inner wall)/W/(m^2 K)	*h*(outer wall)W/(m^2 K)(absolute value)
462	311.3174	638.4426
1640	288.2052	603.5732
4352	271.7196	574.4675
9494	242.0010	512.8537
16,678	238.7773	506.3956
17,084	238.4008	505.3424

the enclosure shape of our study keeps changing during optimization, the mesh number as close to 16,678 as possible was chosen throughout our simulation.

3.5. Computational details and model validation

The commercial CFD code Ansys-Fluent 15.0 that based on the finite volume method is utilized to perform the numerical study. The computational domain is created using the commercial preprocessing code ICEM CFD 15.0. A Lagrangian-Eulerian approach is utilized in the present study. The nanoparticle is tracked using the Lagrangian approach while the governing equations for the base fluid are solved using the Eulerian approach. It is worth noting here that Bianco et al. have compared the accuracy of single phase model and Lagrangian-Eulerian approach in a laminar flow with water-Al_2O_3 [39]. It is reported that the results from both the model are quite similar. Kumar and Puranik [40] studied the convective heat transfer of nanofluids in turbulent flow using a Lagrangian-Eulerian approach. They compared the single phase model with the Lagrangian-Eulerian model and concluded that Lagrangian-Eulerian approach is a more accurate model for simulating forced convection heat transfer when the nanofluid is dilute with the particle volume fraction less than 0.5%. Since the concentrations of nanoparticle in all of our investigated cases are under 0.5%, Lagrangian-Eulerian approach is supposed to be appropriate to simulate the heat transfer process in our cases. The pressure terms in the governing equations are discretized using the second order implicit term, whereas the momentum and energy equations are discretized using the second order upwind scheme. The pressure-velocity coupling is implemented following the SIMPLE algorithm. Additionally, the absolute convergence criterion is set to be 10^{-5} for continuity equation and velocity equation while being 10^{-6} for energy equation. For both water and nanoparticles, Boussinesq approximation is used to simulate natural convection. Typically, pure water is added to the cavity at first where it is under laminar natural convection. Then the nanoparticles are added into water and Eulerian model is used to simulate the two-phase flow.

In order to validate the accuracy of our model and our simulation procedure, the numerical data of the relationship between *Nu* and *Ra* from the literature by Abu-Nada et al. were compared with the simulation of our model [41]. Independent test has been done to find the closest data to the data by Abu-Nada et al. The results are depicted in Fig. 2. As can be seen, there is a good agreement between our simulated results and the previous numerical results.

3.6. Response surface method

RSM is a systematic approach to find the optimal variable that affected by several factors, which combines the numerical method in mathematics and statistics to build models and find a best process for optimization. It is used extensively to find an optimal result meanwhile aiming to save time and cost [42]. There are mainly three steps in response surface method. Firstly, a region that may include the optimal value is ascertained. Secondly, a model is established to describe the relationship between response variable and significant factor. Finally, optimization is conducted in modeling process and the results obtained will be evaluated. When the value is close to the optimal value, a second order model is required to reach response because the real response surface is always curve. In the present study, a second order model is employed to improve accuracy instead of first order model. A general second order model is defined as [43]:

$$y = a_0 + \sum_{i=1}^{n} a_i x_i + \sum_{i=1}^{n} a_{ii} x_i^2 + \sum_{i=1}^{n}\sum_{j=1}^{n} a_{ij} x_i x_j \big|_{i<j} \tag{16}$$

where x_i and x_j are the design variables, a the tuning parameter and n the number of parameters which is 4 in this case. CCD, short of central composite design, adds several design called 'star points' based on first order model and build into a design that has center points. Central composite face-centered design, i.e. CCF, is applied in the present study in which the distance between 'star points' and center point is not equal with the distance between center point and corner point.

In CCF, desirability is an essential function to do optimization, which ranges from 0 to 1.0. The optimal response appears when the value of desirability function reaches 1.0. The optimal value may be reached by adjusting the weight or importance in Eq. (16). In our work, the response is defined as surface heat transfer coefficient. Instead of getting a desirability value of 1.0, the aim of our optimization is to find a series combinations of A and γ that meet all the goals. The simultaneous objective function is a geometric mean of all transformed responses:

$$D = (d_1 \times d_2 \times \cdots \times d_n)^{\frac{1}{n}} = \left(\prod_{i=1}^{n} d_i\right)^{\frac{1}{n}} \tag{17}$$

where n is the number of responses in the measurement and in the present study $n = 1$. In this work, 'Power' is chosen in transformation field and 'maximum' for surface heat transfer coefficient is chosen in the 'goal' field in CCD worksheet. They are defined as follows:

$$\begin{aligned} d_i &= 0, && Y_i \leqslant Low_i \\ d_i &= \left[\frac{Y_i - Low_i}{High_i - Low_i}\right]^{wt_i}, && Low_i < Y_i < High_i \\ d_i &= 1, && Y_i \geqslant High_i \end{aligned} \tag{18}$$

where Y_i is the ith response value and w_t is the weight of that response. Weight can emphasize or deemphasize the target. A weight greater than 1 can emphasize the target while a weight smaller than it will deemphasize the target. In the present work just one response is defined, therefore the weight is inconsequential to final results.

4. Results and discussion

4.1. General effects of WWC shape on its performance

Fig. 3 clearly shows the effect of A and phase deviation γ on surface heat transfer coefficient of WWC (wavy-wavy cavity) containing water-Ag nanofluid. Generally, surface heat transfer coefficient decreases with the increase of A regardless of the phase deviations. However, the influence of phase deviation is also found to be essential for surface heat transfer coefficient if A has been determined. The general heat transfer performance is in the order of $\gamma = 0.5\pi > \gamma = \pi > \gamma = 0.25\pi > \gamma = 0.75\pi$, regardless of the change of A. While for $\gamma = 0$, it is a quite different. For $A = 0.1$, surface heat transfer coefficient for $\gamma = 0$ is the lowest one while it rise to the second when $A = 0.3$. It manifest that the shape of outer boundary has large effect on surface heat transfer coefficient, therefore it is indispensable to find the optimal shape for the outer wavy wall to ensure that the cavity has an enhanced heat transfer efficiency while still maintaining a small overall size.

4.2. Optimal outer wall geometry based on RSM

Fig. 4 shows 3 × 3 temperature contours of the enclosure of various shapes which are all filled with $\varphi = 0.1\%$ Ag nanofluid. In our study, the inner wall shape for the WWC cavity is given, i.e., undulation number of 3 and amplitude of 3 μm. The variation of the temperature contours against non-dimensional amplitude of the outer wall and the phase deviation between the inner and outer walls will be paid special attention. The three figures in each row have the same sinusoidal amplitude A and from the top to the bottom row the non-dimensional amplitude A increases from 0.1 to 0.3. Moreover, the phase deviation between the inner and outer sinusoidal walls increases from 0 to 0.5π and then to π as shown from the left to the right column of Fig. 4, As one can see, one general effect of natural convection in the investigated cavity is that the temperature domain nearby the left adiabatic wall is higher than that of right adiabatic wall. Typically, the isothermal lines are almost parallel to the isothermal walls when $\gamma = 0$. However, the isothermal lines deform and fluctuate much more intensively when $\gamma = 0.5\pi$ and $\gamma = \pi$. On the one hand, as seen from the bottom part of the cavity, the isothermal lines are almost same for the cases of $\gamma = 0$ and $\gamma = 0.5\pi$. It was noticed that near the bottom the shape change of outer wall will not restrict much the development of temperature contour. However, when $\gamma = \pi$, the shape of outer wall become a clear restriction and the isothermal lines become denser, especially for the cases of A = 0.2 and A = 0.3. Clearly, in these cases, the shape of the outer wall of the cavity become dominant for the determination of the temperature distribution in the cavity.

On the other hand, for all the cases, the patterns of the isotherm lines become much more consistent with the shape of the outer walls when they are near the boundaries. From the outer wall to inner wall, one can see a clear phase change for the sinusoidal shape of isotherm lines. It can thus be concluded that in our case the phase deviation is the key parameter for the heat transfer variation of cavity. The larger the amplitude is, the more fluctuated the isotherm will be. Clearly, the sinusoidal amplitude and phase deviation have significant effects on the temperature contours of the WWC, optimization is therefore needed to find optimal outer wall shape with optimal phase deviation between the inner and outer walls of the WWC cavity which leads to the highest significantly improved natural convection heat transfer efficiency.

Response surface method has therefore been employed for the time-efficient optimization of the WWC cavity based on the 9 cases proposed in Fig. 4. As has been mentioned, RSM is a collection of mathematical and statistical techniques, which was applied to establish a mathematical model between independent variable and dependent variable, and find the effect of parameters affecting a response in a process. The time taken to solve the targeted problem can be reduced and a lot of computation resources are saved by using RSM. Generally, the structure of the relationship between the dependent variable and the independent variables is unknown. The first step in RSM is to find a suitable approximation close to the true relationship. The most common forms are low-order polynomials (first or second order). A second-order model can significantly improve the optimization process when a first-order model suffers from some lack of fit due to the interaction between variables and surface curvatures [26]. After our RSM operation over the various cases, the equation of surface heat transfer coefficient can be found by quadratic function and the contours of 2D and 3D results are obtained as shown in Fig. 5. Desirability analysis in Fig. 6 shows that the optimal shape for the outer wavy wall occurs at $A = 0.11$ and $\gamma = 1.77$ rad and the desired surface heat transfer coefficient h reaches to as high as 40360.1 W/(m^2 K) in this case. The desirability for the optimal operating point is about 1.0 which corresponds to a fabulous optimization result. The desirability of 1.0 means that the probability of that case is 100%. It indicates that we will reach to the predicted results by DOE confidently. Validation of the optimization result (Fig. 6(b)) shows that surface heat transfer coefficient of $A = 0.11$ and $\gamma = 1.77$ rad is 40752.62 W/(m^2 K) which is very close to the desired value and verifies the accuracy of RSM method. In the following parts, the effects of various parameters on the performance of the WWC cavity based on this optimized shape will be investigated (see Table 3).

4.3. The effect of volume fractions of nanoparticles

Fig. 7 depicts the evolution of streamlines for the optimized WWC with $A = 0.11$, $\gamma = 1.77$ rad when volume fraction of Ag nanoparticles in the base fluid increases from 0% to 0.9%. Irregular vortex can be clearly seen in the WWC cavity which is almost completely below the central part of the cavity. Typically, for the interior vortex region of the WWC cavity, the low mass flow region which is blue[1] in Fig. 7 becomes smaller and the lower part of this blue region gradually shrinks with the increase of the nanoparticle concentration. The velocity vectors for the streamlines tend to

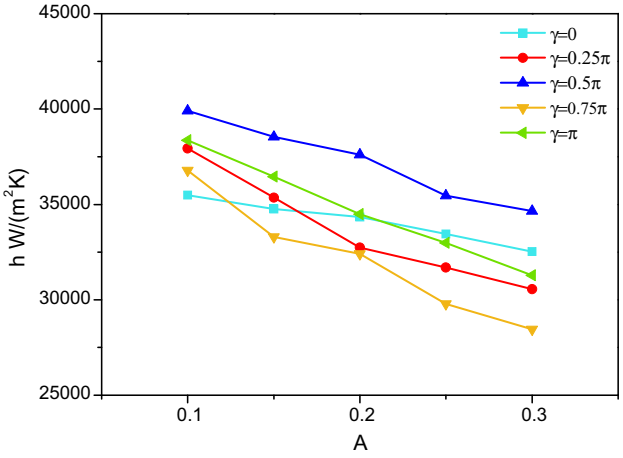

Fig. 3. Effect of non-dimensional sinusoidal amplitude A and phase deviation γ on surface heat transfer coefficient of WWC with $\varphi = 0.1\%$ Ag nanofluid.

[1] For interpretation of color in Fig. 7, the reader is referred to the web version of this article.

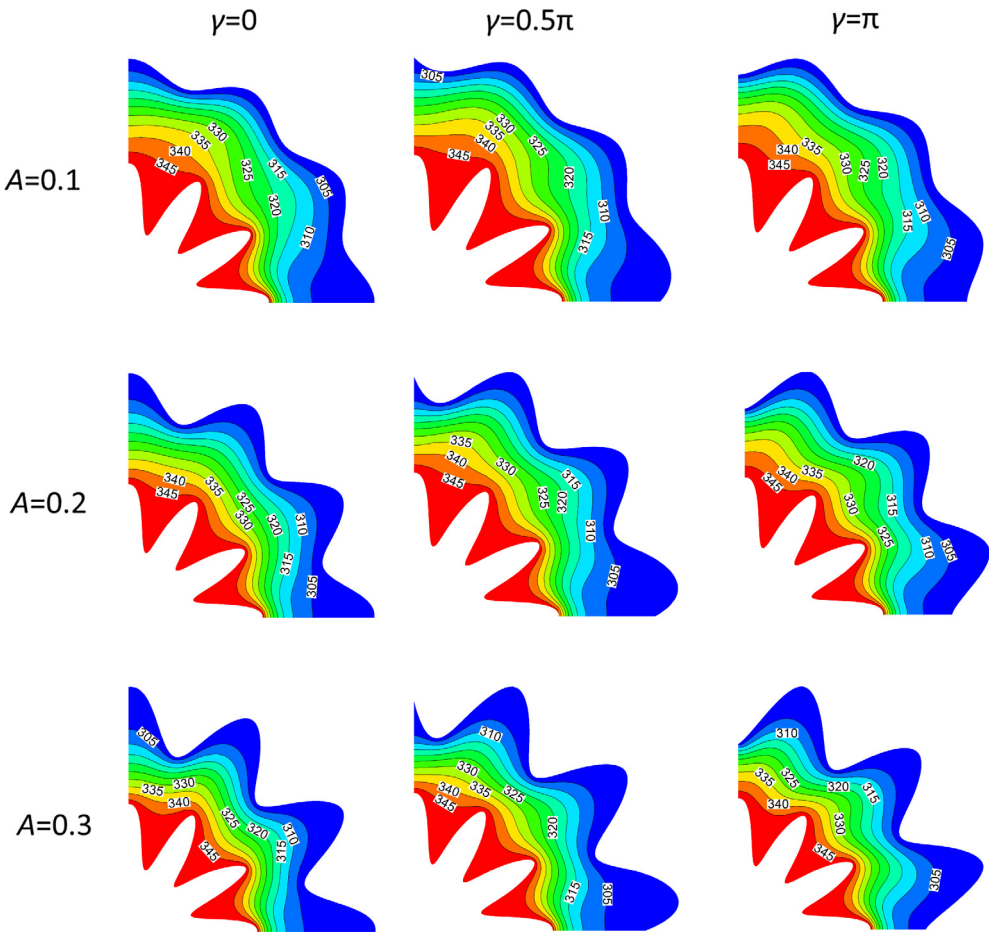

Fig. 4. Temperature contours for 9 cases of WWC with φ = 0.1% Ag nanofluid.

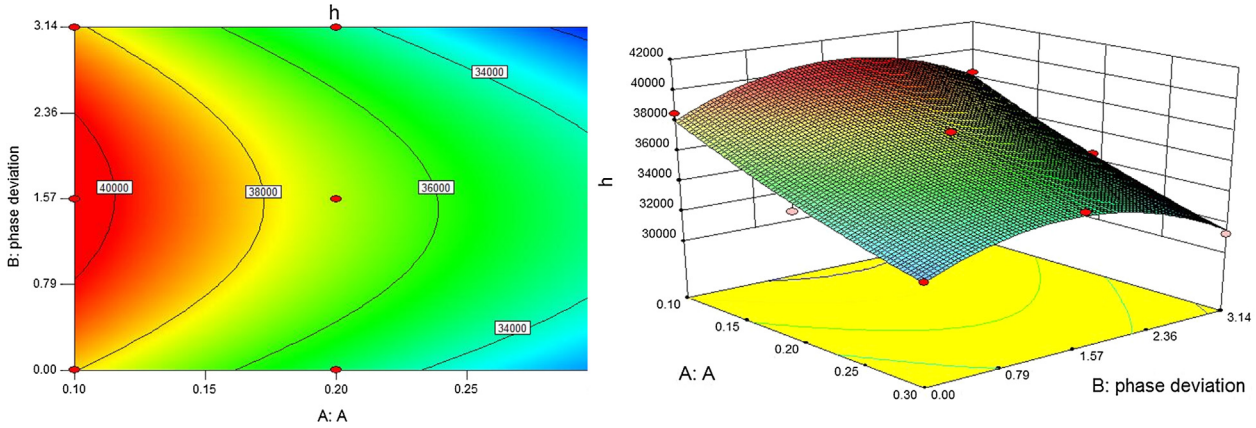

Fig. 5. Effect of sinusoidal amplitude A and phase deviation on surface heat transfer coefficient.

become homogeneous when volume fractions of Ag nanofluids increase from 0% to 0.9%.

It can be seen that for all the cases, the streamlines are generally parallel with each other especially for those near the boundaries of the cavity. Again, it was noticed that the patterns of the streamlines nearby the sinusoidal outer wall become more consistent with its shape. This trend does not change obviously even when the volume fractions of Ag nanofluids increases from 0.1% to 0.9%. However, the interior vortex in the cavity become clearly reduced and deformed with the increase of the Ag nanoparticles. It is worth to mention that the total gravity of nanofluid will increase as the volume fractions of Ag nanofluids increases. The characteristic change for the streamline patterns should therefore be attributed to the increased amount of Ag nanoparticles. It is assumed that with the increase of the nanoparticle concentration the viscosity of the nanofluid will also increase, which in turn leads to a more homogeneous velocity distribution [44]. Surface heat transfer coefficients of Ag nanofluid for the cases when volume fraction increases from 0% to 0.9% is shown in Table 4. It can be seen that the heat transfer coefficients increase rapidly with the increasing

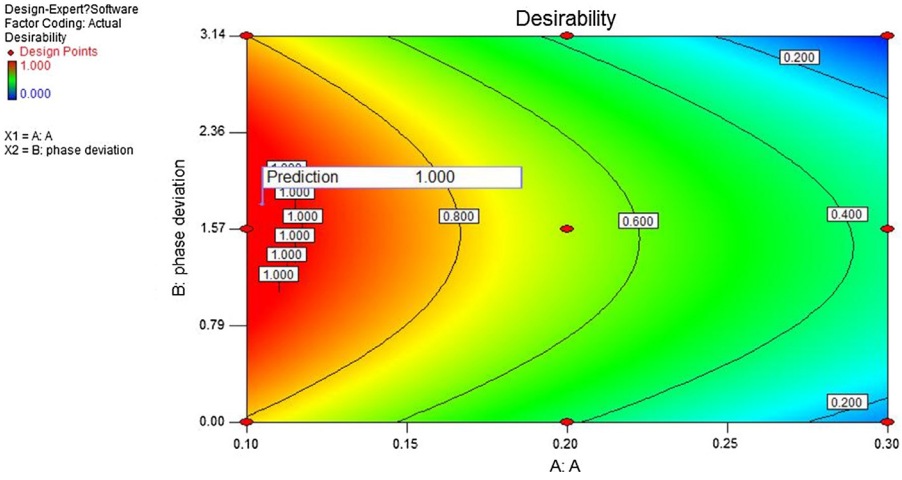

Fig. 6. Desirability function predicting the optimal sinusoidal amplitude *A* and phase deviation for highest surface heat transfer coefficient.

Table 3
RSM for various geometries.

Cases	Ag
$\gamma = 0$, A = 0.1	38512.9
$\gamma = 0$, A = 0.2	34340.2
$\gamma = 0$, A = 0.3	32524.4
$\gamma = 0.5\pi$, A = 0.1	39914.2
$\gamma = 0.5\pi$, A = 0.2	37600.6
$\gamma = 0.5\pi$, A = 0.3	34654.6
$\gamma = \pi$, A = 0.1	38368.6
$\gamma = \pi$, A = 0.2	34487.8
$\gamma = \pi$, A = 0.3	31,280

of Ag nanoparticle volume fractions and notably the increase speed becomes accelerated at higher particle volume fractions.

4.4. The effect of Ra on streamlines

Effect of *Ra* on streamline contour of Ag nanofluids within WWC with $\varphi = 0.1\%$ at $A = 0.11$, $\gamma = 1.77$ rad has also been investigated. In the present work, level of streamline contour is set from 5×10^{-12} to 1.1×10^{-10} kg/s and number of levels is 13. As shown by Fig. 8, *Ra* shows a very significant effect on mass flow rates within the cavity. Generally, with the increase of *Ra*, the flow rate within the cavity shows a rapid increase. In our study, it is considered that

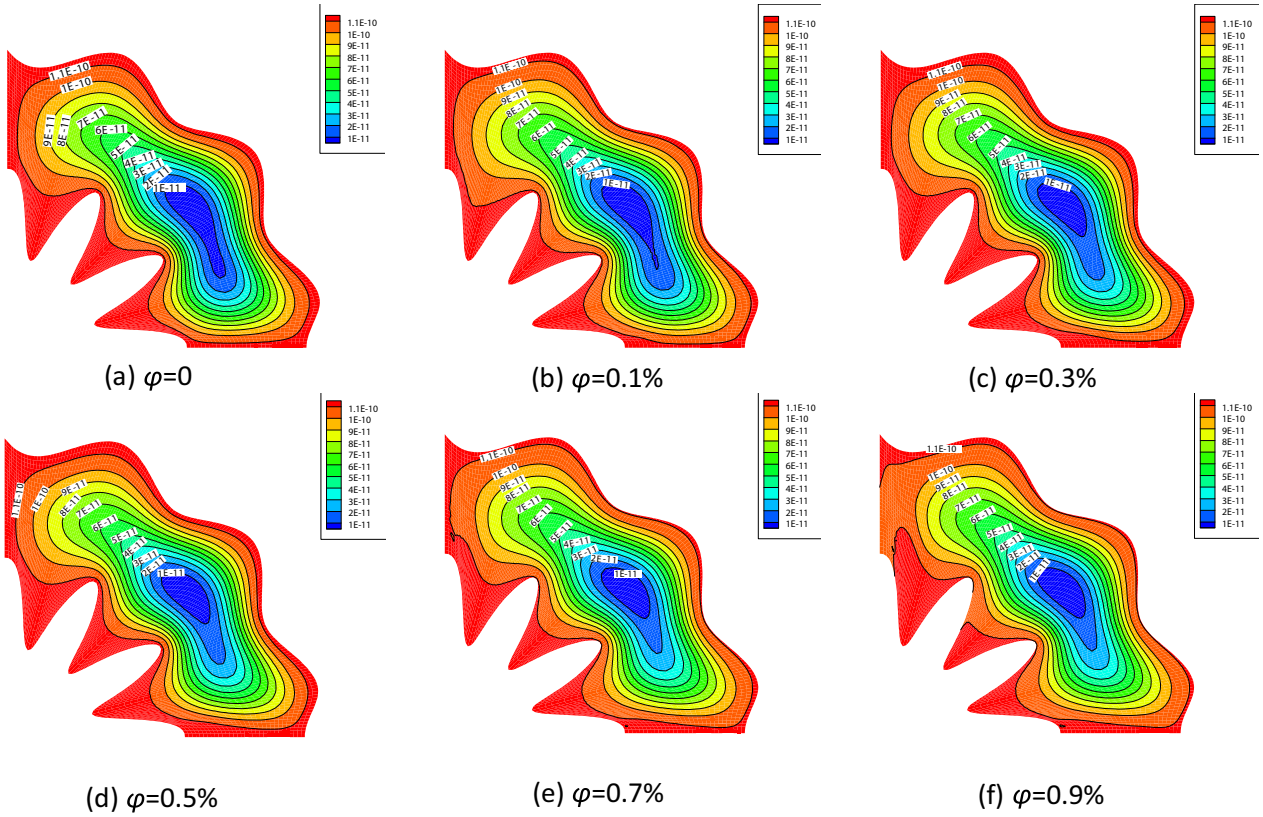

Fig. 7. Streamline evolution of water phase with Ag nanofluids at $A = 0.11$, $\gamma = 1.77$ rad for (a) $\varphi = 0\%$ (b) $\varphi = 0.1\%$ (c) $\varphi = 0.3\%$ (d) $\varphi = 0.5\%$ (e) $\varphi = 0.7\%$ (f) $\varphi = 0.9\%$.

Table 4
Absolute surface heat transfer coefficient of outer wall when of Ag nanofluids at $A = 0.11$, $\gamma = 1.77$ rad for (a) $\varphi = 0\%$ (b) $\varphi = 0.1\%$ (c) $\varphi = 0.3\%$ (d) $\varphi = 0.5\%$ (e) $\varphi = 0.7\%$ (f) $\varphi = 0.9\%$.

	$\varphi = 0$	$\varphi = 0.1\%$	$\varphi = 0.3\%$	$\varphi = 0.5\%$	$\varphi = 0.7\%$	$\varphi = 0.9\%$
$h_{ave}/(W/m^2\,K)$	38811.5	41101.11	44588.64	50133.55	55852.2	64291.73

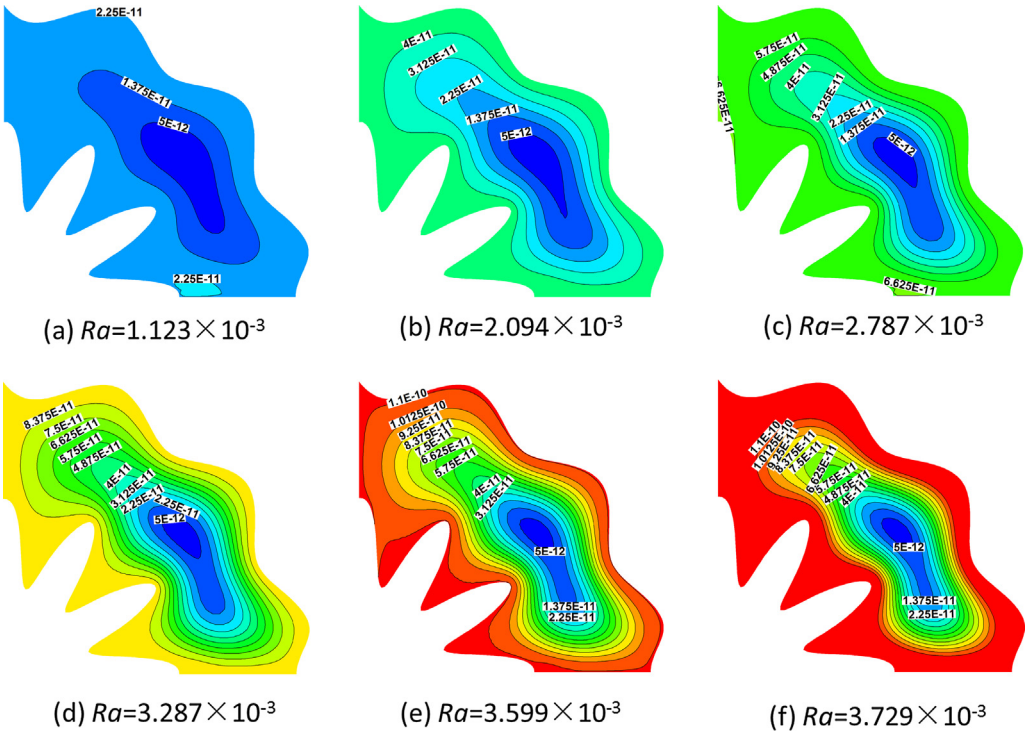

Fig. 8. Effect of Ra on streamline contour of Ag nanofluids within WWC with $\varphi = 0.1\%$ at $A = 0.11$, $\gamma = 1.77$ rad.

Ra can be changed by simply changing the temperature difference of two sinusoidal boundaries. When *Ra* increases from 1.123×10^{-3} to 3.729×10^{-3}, streamline become denser due to the increasing temperature differences. Obviously, in our case, the temperature difference between two sinusoidal boundaries should be the main driving force for the accelerated movements of nanoparticles as well as base fluid in the cavity. Therefore it is suggested that in order to enhance heat transfer, the *Ra* number could be as high as possible if the material of the cavity can withstand such thermal loading.

4.5. Effects of nanofluids and comparison with CWC

In this part, we investigated the effect of different kinds of nanofluid on the performance of the WWC (wavy-wavy cavity) based on its optimized shape and compared it with WWC (circular-wavy cavity) under same working conditions. Fig. 9 shows different performances of four typical kinds of nanofluid, i.e., water-Ag, water-CuO, water-Al_2O_3 and water-TiO_2. The general heat transfer performance is in the order of water-Ag > water-CuO > water-Al_2O_3 > water-TiO_2. Obviously, Ag nanofluid shows the best performance. As has been demonstrated experimentally, Ag should have higher thermal diffusivity than many metal oxides especially due to its small particle sizes [45]. Apparently, our results indicate that it is the inherent properties of Ag nanoparticles instead of the cavity geometry which leads to its high heat transfer performance.

Furthermore, the performance of our optimized WWC cavity was compared with the previously reported CWC cavity [23]. Here

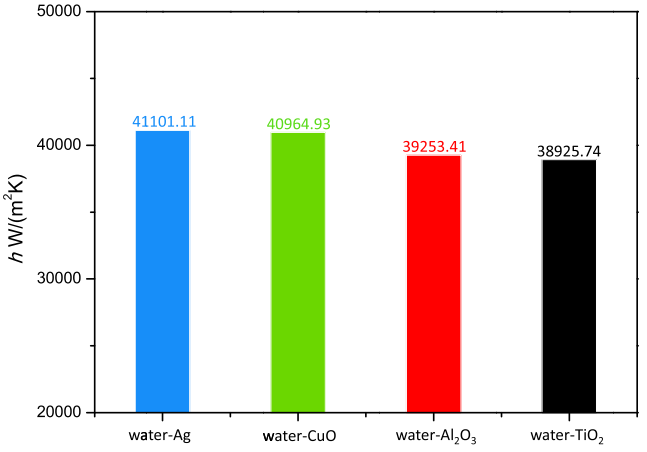

Fig. 9. Comparison of absolute surface heat transfer coefficient of water-Ag, water-CuO, water-Al_2O_3, water-TiO_2, respectively, for WWC when $\varphi = 0.1\%$ at $A = 0.11$, $\gamma = 1.77$ rad.

for both cavities, *A* and *N* of inner wall keeps to be 0.3 and 9, respectively. As shown by Fig. 10, for both cases there is a general increasing tendency of local Nusselt number with the increasing of rotation angel. For the CWC cavity, the increase is almost a lineal one. However, for the WWC cavity, a periodical fluctuation of local Nusselt number at different locations of the outer wavy wall can be clearly found. The general trend is that the increase of the Nusselt number is always larger than the following decrease and the net

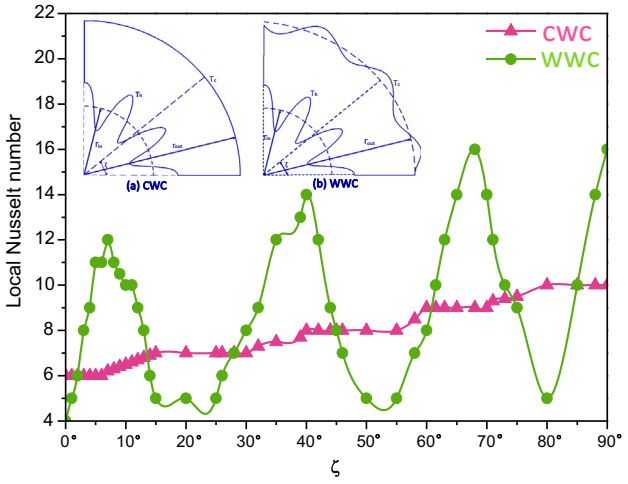

Fig. 10. Comparison of local Nusselt numbers for (a) CWE with (b) WWE cavities at different rotation angles, φ = 0.1% Ag nanofluid at A = 0.11, γ = 1.77 rad.

result is that the outer wall Nusselt number is evidently larger than that of CWC. It is worth noted that such fluctuated variation of natural convection heat transfer at cavity surface should be of particular interest for some special applications such as for the cooling of electronic device of irregular shape which also has an uneven temperature distribution.

5. Conclusions

In the present work, a new geometry with double sinusoidal wavy walls of various phase deviations has been proposed for natural convection heat transfer. This study has systematically considered the effect of phase deviation of two sinusoidal walls and heat transfer property of four nanofluids in a cavity under natural convection. Finite volume method (FVM) was applied to solve the non-dimensional governing equations together with the specified boundary conditions. RSM combined with FVM was employed to optimize the performance of the proposed geometry. Computational results of temperature and velocity within the cavity are shown graphically. The important conclusions from our study are summarized as below:

1. The phase deviation can largely influence heat transfer coefficient. The general heat transfer performance is in the order of $\gamma = 0.5\pi > \gamma = \pi > \gamma = 0.25\pi > \gamma = 0.75\pi$, regardless of the change of A.
2. The RSM results indicate that when the shape of inner wall is given as A = 0.3 and N = 9, the optimal shape for the outer wall is A = 0.11 and phase deviation γ = 1.77 rad.
3. The surface heat transfer coefficient increases significantly when the volume fraction of nanofluid increases and the large volume fraction makes temperature distribution within cavity more homogeneous.
4. Among the four kinds of nanofluids investigated, water-Ag nanofluid has the best performance. The heat transfer performance is in the order of water-Ag > water-CuO > water-Al_2O_3 > water-TiO_2.
5. For the WWC cavity, a periodical fluctuation of local Nusselt number at different locations of the outer wavy wall has been found and the net result is that the outer wall Nusselt number is evidently larger than that of CWC.

Acknowledgments

The authors gratefully acknowledge the financial support of the National Natural Science Foundation of China (No. 51422604) and the National 863 Program of China (No. 2013AA050402). This work was also supported by the China Fundamental Research Funds for the Central Universities.

Conflict of interest

We declare that we have no financial and personal relationships with other people or organizations that can inappropriately influence our work, there is no professional or other personal interest of any nature or kind in any product, service and/or company that could be construed as influencing the position presented in, or the review of, the manuscript entitled.

References

[1] S. Ostrach, Natural convection in enclosures, J. Heat Transf. 110 (1988) 1175–1190.
[2] W.I. Moore, E.S. Donovan, C.R. Powers, Thermal analysis of automotive lamps using the ADINA-F coupled specular radiation and natural convection model, Comput. Struct. 72 (1999) 17–30.
[3] B. Li, C. Byon, Investigation of natural convection heat transfer around a radial heat sink with a concentric ring, Int. J. Heat Mass Transf. 89 (2015) 159–164.
[4] B. Singh, S.K. Dash, Natural convection heat transfer from a finned sphere, Int. J. Heat Mass Transf. 81 (2015) 305–324.
[5] S.T. Mohyud-Din, Z.A. Zaidi, U. Khan, N. Ahmed, On heat and mass transfer analysis for the flow of a nanofluid between rotating parallel plates, Aerosp. Sci. Tech. 46 (2015) 514–522.
[6] N. Ahmed, S.T. Mohyud-Din, S.M. Hassan, Flow and heat transfer of nanofluid in an asymmetric channel with expanding and contracting walls suspended by carbon nanotubes: a numerical investigation, Aerosp. Sci. Tech. 48 (2016) 53–60.
[7] S.Z.A. Zaidi, S.T. Mohyud-Din, Convective heat transfer and MHD effects on two dimensional wall jet flow of a nanofluid with passive control mode, Aerosp. Sci. Tech. 49 (2016) 225–230.
[8] H. Sajjadi, M. Gorji, G.H.R. Kefayati, D.D. Ganji, Lattice Boltzmann simulation of turbulent natural convection in tall enclosures using Cu/water nanofluid, Numeri. Heat Transf. A 62 (2012) 512–530.
[9] G.R. Kefayati, Lattice Boltzmann simulation of natural convection in nanofluid-filled 2D long enclosures at presence of magnetic field, Theor. Comput. Dyn. 27 (2013) 865–883.
[10] G.R. Kefayati, Effect of a magnetic field on natural convection in an open cavity subjugated to Water/Alumina nanofluid using lattice Boltzmann method, Int. Commun. Heat Mass Transf. 40 (2013) 67–77.
[11] G.R. Kefayati, Simulation of ferrofluid heat dissipation effect on natural convection at an inclined cavity filled with kerosene/cobalt utilizing the Lattice Boltzmann method, Numer. Heat Transf. A 65 (2014) 509–530.
[12] G.R. Kefayati, FDLBM simulation of entropy generation due to natural convection in an enclosure filled with non-Newtonian nanofluid, Powder Technol. 273 (2015) 176–190.
[13] G.R. Kefayati, R.R. Huilgol, Lattice Boltzmann Method for simulation of mixed convection of a Bingham fluid in a lid-driven cavity, Int. J. Heat Mass Transf. 103, 725–743.
[14] G.R. Kefayati, Heat transfer and entropy generation of natural convection on non-Newtonian nanofluids in a porous cavity, Powder Technol. 299 (2016) 127–149.
[15] G.R. Kefayati, H. Tang, Simulation of natural convection and entropy generation of non-Newtonian nanofluid in a porous cavity using Buongiorno's mathematical model, Int. J. Heat Mass Transf. 112 (2017) 709–744.
[16] U. Khan, N. Ahmed, S.T. Mohyud-Din, Analysis of magnetohydrodynamic flow and heat transfer of Cu-water nanofluid between parallel plates for different shapes of nanoparticles, Neural Comp. Appl. (2016) 1–9.
[17] U. Khan, N. Ahmed, S.T. Mohyud-Din, B. Bin-Mohsin, Nonlinear radiation effects on MHD flow of nanofluid over a stretching/shrinking wedge, Neural Comp. Appl. (2016) 1–10.
[18] N. Ahmed, U. Khan, Z.A. Zaidi, S.U. Jan, A. Waheed, MHD flow of an incompressible fluid through porous medium between dilating and squeezing permeable walls, J. Porous Media 17 (10) (2014) 861–867.
[19] G.R. Kefayati, Lattice Boltzmann simulation of MHD natural convection in a nanofluid-filled cavity with sinusoidal temperature distribution, Powder Technol. 243 (2013) 171–183.
[20] G.R. Kefayati, Simulation of heat transfer and entropy generation of MHD natural convection of non-Newtonian nanofluid in an enclosure, Int. J. Heat Mass Transf. 92 (2016) 1066–1089.
[21] U. Khan, N. Ahmed, S.T. Mohyud-Din, Heat transfer effects on carbon nanotubes suspended nanofluid flow in a channel with non-parallel walls

under the effect of velocity slip boundary condition: a numerical study, Neural Comput. Appl. (2015) 1–10.
[22] U. Khan, N. Ahmed, S.T. Mohyud-Din, Numerical Investigation for three dimensional squeezing flow of nanofluid in a rotating channel with lower stretching wall suspended by carbon nanotubes, Appl. Therm. Eng. 113 (2017) 1107–1117.
[23] M. Hatami, D. Song, D. Jing, Optimization of a circular-wavy cavity filled by nanofluid under the natural convection heat transfer condition, Int. J. Heat Mass Transf. 98 (2016) 758–767.
[24] M. Sheikholeslami, M. Gorji-Bandpy, D.D. Ganji, S. Soleimani, MHD natural convection in a nanofluid filled inclined enclosure with sinusoidal wall using CVFVM, Neural Comput. Appl. 24 (2014) 873–882.
[25] M.A. Sheremet, I. Pop, H.F. Öztop, N. Abu-Hamdeh, Natural convective heat transfer and nanofluid flow in a cavity with top wavy wall and corner heater, J. Hydrodyn. B 28 (2016) 873–885.
[26] S.Y. Motlagh, H. Soltanipour, Natural convection of Al_2O_3-water nanofluid in an inclined cavity using Buongiorno's two-phase model, Int. J. Therm. Sci. 111 (2017) 310–320.
[27] G.R. Kefayati, Mixed convection of non-Newtonian nanofluid in an enclosure using Buongiorno's mathematical model, Int. J. Heat Mass Transf. 108 (2017) 1481–1500.
[28] D.H. Yoo, K.S. Hong, H.S. Yang, Study of thermal conductivity of nanofluids for the application of heat transfer fluids, Thermochim. Acta 455 (2007) 66–69.
[29] H. Cui, F. Xu, S.C. Saha, A three-dimensional simulation of transient natural convection in a triangular cavity, Int. J. Heat Mass Transf. 85 (2015) 1012–1022.
[30] J. Rostami, A. Abbassi, M. Saffar-Avval, Optimization of conjugate heat transfer in wavy walls microchannels, Appl. Therm. Eng. 82 (2015) 318–328.
[31] Q. Deng, J. Chang, Natural convection in a rectangular enclosure with sinusoidal temperature distributions on both side walls, Numer Heat Transf. A 54 (2008) 507–524.
[32] A.I. Alsabery, A.J. Chamkha, S.H. Hussain, H. Saleh, I. Hashim, Heatline visualization of conjugate natural convection in a square cavity filled with nanofluid with sinusoidal temperature variations on both horizontal walls, Int. J. Heat Mass Transf. 100 (2016) 835–850.
[33] J. Zhou, M. Hatami, D. Song, D. Jing, Design of microchannel heat sink with wavy channel and its time-efficient optimization with combined RSM and FVM methods, Int. J. Heat Mass Tranf. 103 (2016) 715–724.
[34] Ansys-Fluent Documentation, Theory Guide, User Guide, Release 14 (2011) 5.
[35] Y. He, Y. Men, Y. Zhao, H. Lu, Y. Ding, Numerical investigation into the convective heat transfer of TiO_2 nanofluids flowing through a straight tube under the laminar flow conditions, Appl. Therm. Eng. 29 (2009) 1965–1972.
[36] K. Apostolou, A.N. Hrymak, Discrete element simulation of liquid-particle flows, Comput. Chem. Eng. 32 (2008) 841–856.
[37] P.G. Staffman, The lift on a small sphere in a slow shear flow, J. Fluid Mech. 22 (1965) 385–400.
[38] M. Sheikholeslami, M. Gorji-Bandpy, D.D. Ganji, Soheil Soleimani, Natural convection heat transfer in a cavity with sinusoidal wall filled with CuO-water nanofluid with the presence of magnetic field, J. Taiwan Inst. Chem. E 45 (2014) 40–49.
[39] V. Bianco, F. Chiacchio, O. Manca, S. Nardini, Numerical investigation of nanofluids forced convection in circular tubes, Appl. Therm. Eng. 29 (2009) 3632–3642.
[40] N. Kumar, B.P. Puranik, Numerical study of convective heat transfer with nanofluid in turbulent flow using a Lagrangian-Eulerian approach, Appl. Therm. Eng. 111 (2017) 1674–1681.
[41] E. Abu-Nada, Z. Masoud, A. Hijazi, Natural convection heat transfer enhancement in horizontal concentric annuli using nanofluids, Int. Commun. Heat Mass Transf. 35 (2008) 657–665.
[42] M. Rahimi-Gorji, O. Pourmehran, M. Hatami, D.D. Ganji, Statistical optimization of microchannel heat sink (MCHS) geometry cooled by different nanofluids using RSM analysis, Eur. Phys. J. Plus 130 (2015) 1–21.
[43] S.J. Yaseen, numerical study of steady natural convection flow in a prismatic enclosure with strip heater on bottom wall using flexpde, Diyala J. Eng. Sci. 7 (2014) 61–80.
[44] Z. Ling, D. Sun, Z.Q. Zhang, Effects of temperature and particle concentration on viscosity of nanofluids, Funct. Mater. 44 (2013) 92–95.
[45] M.H. Esfe, S. Saedodin, M. Biglari, H. Rostamian, An experimental study on thermophysical properties and heat transfer characteristics of low volume concentrations of Ag-water nanofluid, Int. Commun. Heat Mass Transf. 74 (2016) 91–97.